LA-UR-1226

Approved for public release;
distribution is unlimited.

Title: GEANT simulations for the neutron absorber at DANCE

Author(s): R. Reifarth, E.-I. Esch, LANSCE-3, LANL

Submitted to: DANCE collaboration

Los Alamos
NATIONAL LABORATORY

Los Alamos National Laboratory, an affirmative action/equal opportunity employer, is operated by the University of California for the U.S. Department of Energy under contract W-7405-ENG-36. By acceptance of this article, the publisher recognizes that the U.S. Government retains a nonexclusive, royalty-free license to publish or reproduce the published form of this contribution, or to allow others to do so, for U.S. Government purposes. Los Alamos National Laboratory requests that the publisher identify this article as work performed under the auspices of the U.S. Department of Energy. Los Alamos National Laboratory strongly supports academic freedom and a researcher's right to publish; as an institution, however, the Laboratory does not endorse the viewpoint of a publication or guarantee its technical correctness.

Form 836 (8/00)

GEANT simulations for the neutron absorber at DANCE

R. Reifarth* and E.-I. Esch*

*Los Alamos National Laboratory, Los Alamos, New Mexico, 87545, USA

Abstract. GEANT simulations have been performed to investigate the impact of filling the holes in the neutron absorber shell inside the DANCE array. The simulations have shown that it is not necessary to buy the expensive ^{6}LiH plugs, but that plugs made of the much cheaper $^6Li_2CO_3$ have a similar effect.

1. INTRODUCTION

One of the most important backgrounds during neutron capture cross section measurements with DANCE is caused by scattered neutrons, which eventually get captured in the BaF_2 crystals or other structural components. In order to reduce this background, a ^{6}LiH sphere has been designed to absorb the scattered neutron on their way from the sample to the detector. The first design of DANCE included a sample changing mechanism, which was positioned perpendicular to the neutron beam. The ^{6}LiH sphere therefore contained not only holes for the beam pipe, but also 2 additional holes of 5 cm diameter under 90° (see [1] for more details).

The 6 cm thick layer of ^{6}LiH is especially effective for neutron energies below 1 keV. The two additional holes are therefore determining the neutron induced background during the measurements with DANCE. This report quantifies this statement and describes possible solutions, which do not necessarily involve the rather expensive purchase of custom-made plugs out of ^{6}LiH, but the significantly cheaper $^6Li_2CO_3$. More details on the simulation technique can be found in previous reports [2, 3, 4].

1.1. Colors and directions

Fig. 1 shows a colored representation of the crystal ball according to the crystal numbers. The left part corresponds to 3D drawings made with the GEANT graphics package [5], where the lowest crystal numbers are drawn in white. The intermediate crystal numbers are shown in black, red, green, dark blue, yellow, and purple. The highest numbers correspond to light blue. The crystal numbering scheme starts with 0 at the right hand side, if looking in beam direction, and continuous in spirals around the axis between crystal 0 and the opposite crystal 162 to the left hand side. The right part of Fig. 1 contains the same information, but in a 2D-plot, where ϑ and φ are the angles in spherical coordinates.

Fig. 2 shows the results of a neutron simulation in the same way as explained for Fig. 1. Now the colors correspond to the number of counts per detector. The details of this and the following 2 simulation will be described in section 2.2. The most important feature to recognize is that for isotropically emitted neutrons, the number of counts per detector is not the same for each detector. The simulated geometry included the two holes in the ^{6}LiH shell in front of detector 31 and 121. Those are the two detectors with the highest count rates. Obviously the two holes in the absorber sphere are dominating the neutron induced background.

Fig. 3 shows the results for a simulation with the same parameters as for Fig. 2, but the holes in the absorber sphere are filled with ^{6}LiH, which means the absorber sphere is now homogeneous except for the two holes for the neutron beam pipe. According to a quote from the manufacturer, the costs for the required plugs would be around USD 50k. The result of such plugs is a dramatic reduction of the count rate in the equatorial plane, especially around crystals 31 and 121. Only the crystals nearest to the beam axis still show an enhanced count rate, since they are not as well shielded as the other ones.

Fig. 4 shows the results for a simulation with the same parameters as for Fig. 2, but the holes in the absorber sphere are filled with 3.5 cm $^6Li_2CO_3$. This solution has the advantage of being significantly cheaper (less than USD 1k), but

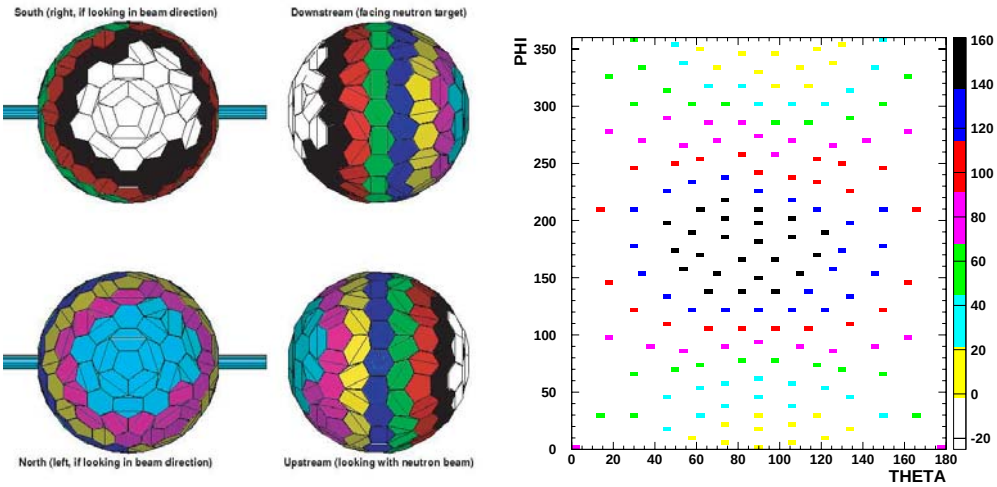

FIGURE 1. **Left:** Schematic view of the DANCE array. The colors are according to crystal numbers 0 .. 162. The order of the colors are (from lowest) white, black, red, green, dark blue, yellow, purple, and light blue. **Right:** The 2D-plot contains the same information as the pictures on the left, but as a $\vartheta - \varphi$-plot.

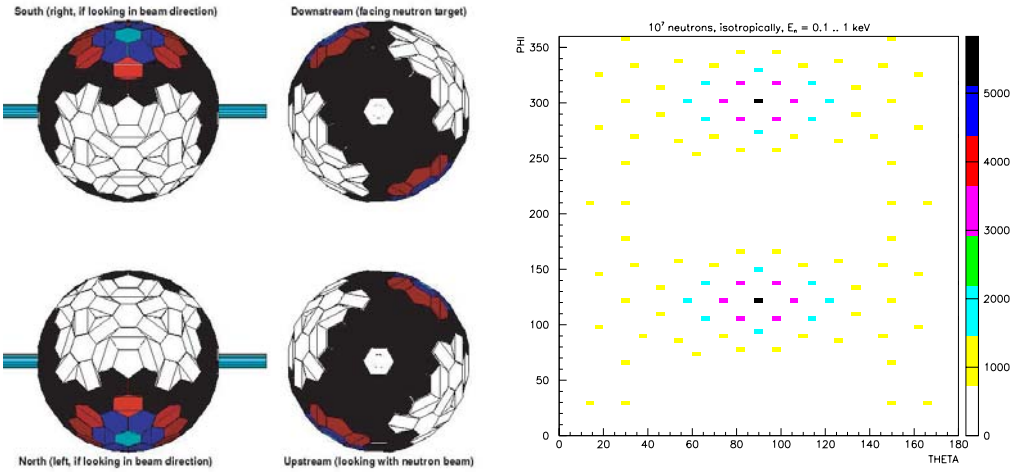

FIGURE 2. The color code in this figure is the same as in Fig. 1, but the colors correspond to the count rate in a single detector. The counts in the detector are caused by neutron between 0.1 and 1 keV, which were isotropically emitted in the center of the DANCE array. The simulation included the holes in the neutron absorber sphere, which was the status of the DANCE array until January 2004 (see section 2.2 for details).

has the disadvantage of being less effective in absorbing neutrons. Furthermore, the interaction probability for γ-rays is significantly higher, if the thickness would be chosen to have the same neutron absorption quality. The simulated thickness of 3.5 cm is therefore a compromise between absorbing as many neutron as possible and being as transparent as possible for γ-rays. More details on the interaction probability for γ-rays are given in section 3. The effect of such plugs will be discussed in detail in the next section, but it is already clear at this point, that the count rate for the detectors around detector 31 and 121 are significantly reduced.

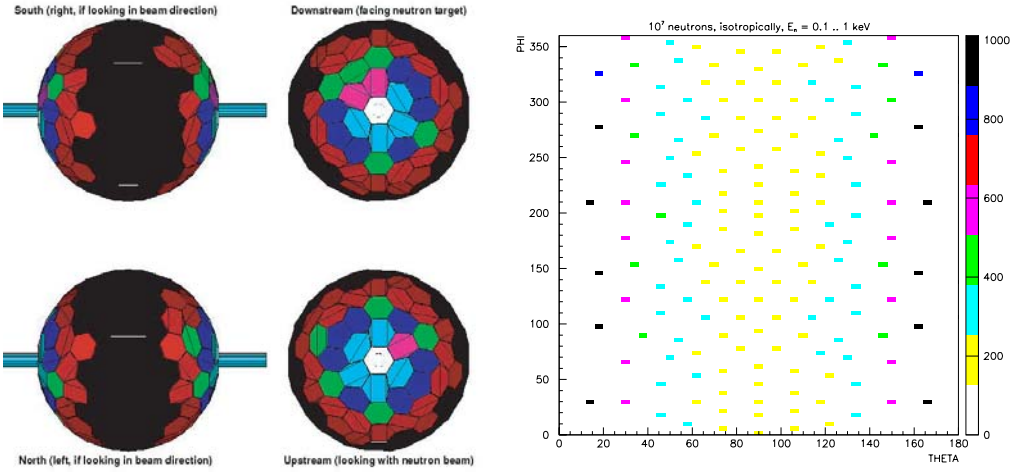

FIGURE 3. The color code in this figure is the same as in Fig. 1, but the colors correspond to the count rate in a single detector. The counts in the detector are caused by neutron between 0.1 and 1 keV, which were isotropically emitted in the center of the DANCE array. The simulation assumed ^{6}LiH plugs in the absorber sphere (see section 2.2 for details).

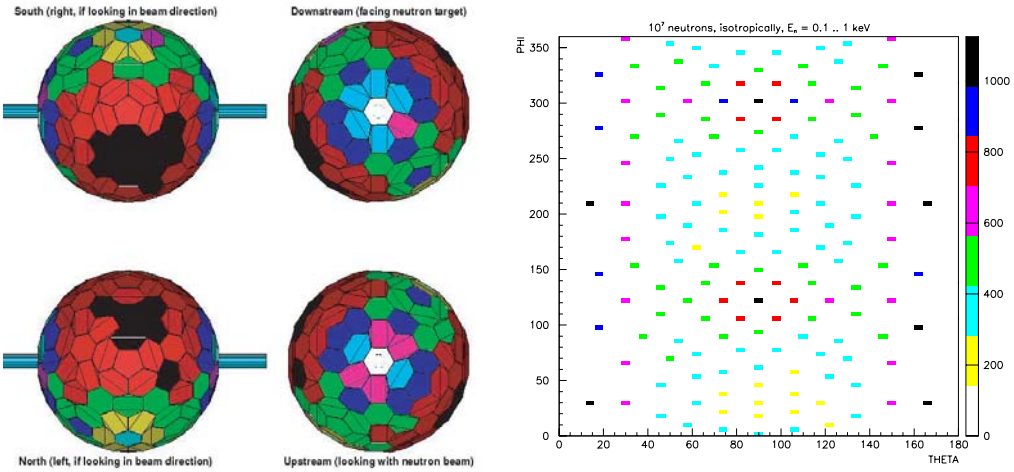

FIGURE 4. The color code in this figure is the same as in Fig. 1, but the colors correspond to the count rate in a single detector. The counts in the detector are caused by neutron between 0.1 and 1 keV, which were isotropically emitted in the center of the DANCE array. The simulation assumed 3.5 cm $^{6}Li_2CO_3$ plugs in the absorber sphere (see section 2.2 for details).

TABLE 1. Number of events caused by 10^6 neutrons in the interval 1 .. 10 eV as a function of the energy deposition in the DANCE array. The energy region above 4 MeV is most important for the experiments at DANCE.

Geometry	Total sum	Sum above 1 MeV	Sum above 4 MeV
holes in LiH	$4.22\ 10^3$	$4.00\ 10^3$	$3.20\ 10^3$
plugs in LiH	$1.19\ 10^3$	$1.04\ 10^3$	$6.40\ 10^2$
no holes in LiH	$1.18\ 10^3$	$1.04\ 10^3$	$6.42\ 10^2$

2. THE NEUTRON ABSORBER AND NEUTRONS

This section describes in detail the simulations carried out with different geometries and different neutron energies in order to find to optimal compromise for filling the holes in the ^{6}LiH neutron absorber of the DANCE array. The ^{6}LiH shell used during the experiments at DANCE has an inner radius of 10.5 cm and an outer radius of 16.5 cm. Due to outdated design requirements, the sphere contains not only holes for the neutron beam pipe, but also holes for a sample changing mechanism, which are perpendicular to the beam pipe holes. All holes have a diameter of 5.08 cm (2 inches). The following sections compare always 3 different setups:

1. "holes in LiH" - contains the neutron beam pipe holes as well as the 2 additional holes in the ^{6}LiH shell.
2. "plugs in LiH" - contains the neutron beam pipe holes and 3.5 cm $^6Li_2CO_3$ plugs inside the 2 additional holes in the ^{6}LiH shell. The plugs are positioned at the outer end of the ^{6}LiH shell.
3. "full LiH" - contains the neutron beam pipe holes and no additional holes in the ^{6}LiH shell. In practice that would mean 6 cm long plugs out of ^{6}LiH inside the shell.

2.1. Low neutron energies

The runs in this subsection are simulated with neutrons in the energy range between 1 and 100 eV. This is the region of resolved resonances and is often used for nuclear structure studies as well as the determination of so-called epithermal cross sections. An environment, free of background from scattered neutron is highly desirable, since the regions between the capture resonances are often accompanied by fairly large scattering cross sections.

The neutron distribution within each run followed a $1/E_n$ spectrum, as it is typical for a spallation source. The additional plugs are most effective for low neutron energies. A reduction of the overall count rate due to neutrons, which are scattered off the sample, up to a factor of five in the energy region of interest was observed. Furthermore, the difference between the less effective, but cheaper $^6Li_2CO_3$ plugs and the ^{6}LiH plugs are only marginal.

2.1.1. Events per Detector

Figs. 5 and 6 show the total number of counts per detector for the neutron energy interval 1-10 eV and 10-100 eV, respectively. Especially the number of counts in the detectors 31, 121 and their neighbors is largely reduced. The right part of each figure shows only the comparison between the two plugs.

Not the entire sum-energy region of the DANCE spectrum is interesting for data analysis. Most of the isotopes under investigation have neutron capture Q-values of more than 4 MeV. Table 1 contains therefore the total number of counts in different sum-energy regions for neutrons between 1 and 10 eV. Table 2 shows the same data, but normalized to the run with $^6Li_2CO_3$ plugs. Especially for the higher sum-energies, the region of interest for (n,γ) measurements at DANCE, the $^6Li_2CO_3$ plugs are very effective and there is basically no difference between the $^6Li_2CO_3$ and the ^{6}LiH plugs.

Tables 3 and 4 show the results for neutrons between 10 and 100 eV. The effect of the $^6Li_2CO_3$ is similar for this neutron energy range as for the one above.

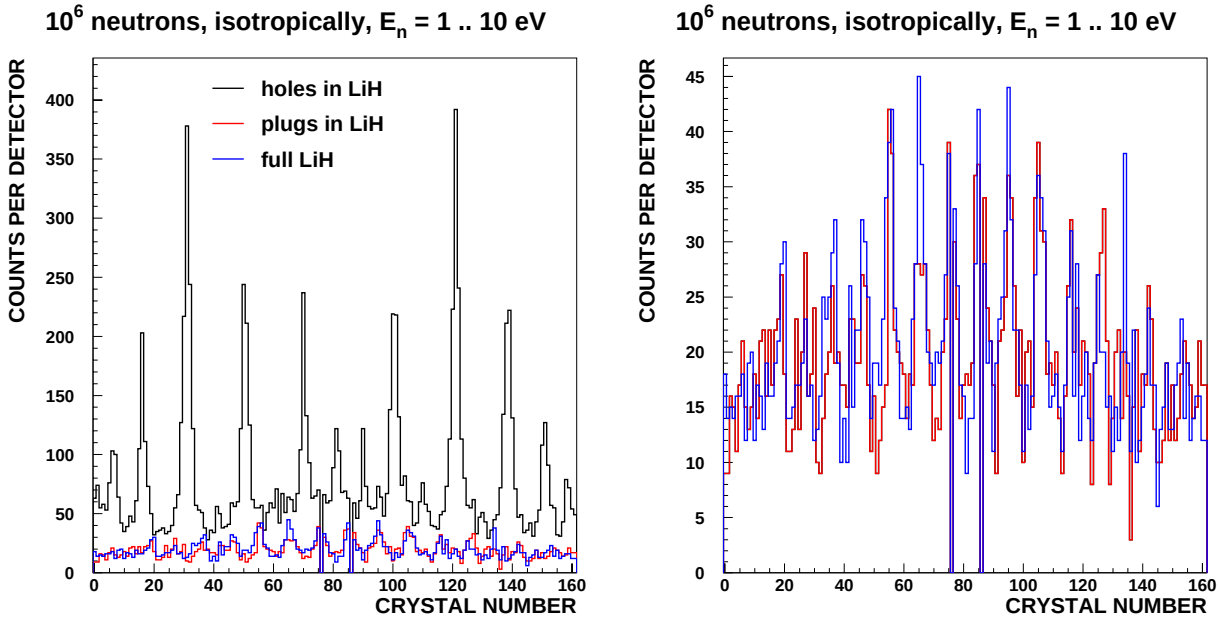

FIGURE 5. Number of events per detector for the neutron energy range 1 .. 10 eV for different geometries. The black curve corresponds to the setup as during the run 2004, where the neutron absorber contained holes for the sample changer. The red curve corresponds the a run with a plug of 3.5 cm $^6Li_2CO_3$ to fill the holes. Finally, the blue curve shows the result for a run with a plug of ^{6}LiH to fill the holes.

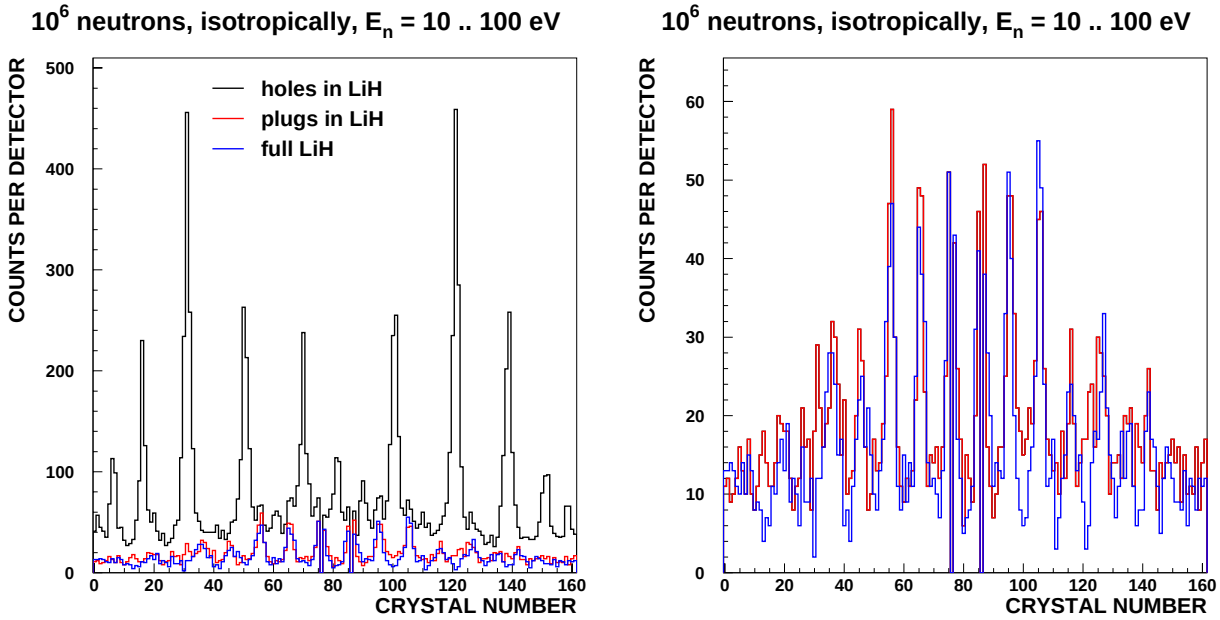

FIGURE 6. Number of events per detector for the neutron energy range 10 .. 100 eV for different geometries. The black curve corresponds to the setup as during the run 2004, where the neutron absorber contained holes for the sample changer. The red curve corresponds the a run with a plug of 3.5 cm $^6Li_2CO_3$ to fill the holes. Finally, the blue curve shows the result for a run with a plug of ^{6}LiH to fill the holes.

TABLE 2. Ratio of events caused neutrons in the interval 1 .. 10 eV as a function of the energy deposition in the DANCE array. All numbers are relative to to the run with $^6Li_2CO_3$ plugs inside the ^{6}LiH neutron absorber, see Table 1 for absolute numbers.

Geometry	Total ratio	Ratio above 1 MeV	Ratio above 4 MeV
holes in ^{6}LiH	3.55	3.85	5.00
plugs in ^{6}LiH	1	1	1
no holes in ^{6}LiH	0.99	1.00	1.00

TABLE 3. Number of events caused by 10^6 neutrons in the interval 10 .. 100 eV as a function of the energy deposition in the DANCE array. The energy region above 4 MeV is most important for the experiments at DANCE.

Geometry	Total sum	Sum above 1 MeV	Sum above 4 MeV
holes in LiH	$3.63\ 10^3$	$3.46\ 10^3$	$2.85\ 10^3$
plugs in LiH	$1.10\ 10^3$	$9.90\ 10^2$	$6.46\ 10^2$
no holes in LiH	$1.01\ 10^3$	$8.75\ 10^2$	$5.58\ 10^2$

2.1.2. Media and isotopes capturing neutrons

In order to understand to cause and possibly find further reduction of the background due to scattered neutrons, a analysis of the parts, where the neutrons get eventually captured, is very helpful. Within the GEANT framework different volumes can be made of different media, where a medium is typically a mixture of different materials. All the crystals, for instance, are made of medium 2, which is BaF_2, while medium 2 itself is a mixture of the materials barium and fluoride.

The following media where used during the simulations:

- 1 .. air, surrounding the beam pipe as well as the DANCE array
- 2 .. BaF_2, all 160 crystals
- 5 .. vacuum, inside the beam pipe
- 6 .. PVC, covers the BaF_2 crystals
- 8 .. Al, the supporting structure holding the crystals in place
- 9 .. PM, a mixture containing the material used inside the photomultiplier tubes.
- 12 .. ^{6}LiH, material for the neutron absorber shell
- 16 .. Al alloy, neutron beam pipe
- 17 .. $^6Li_2CO_3$, plugs to fill the holes inside the absorber shell

The two top panels of Fig. 7 show the number of neutron captures as a function of the medium number. In the case of holes in the absorber sphere, most of the neutron captures occur inside the crystals (BaF_2). This situation changes, as soon as the holes are filled with one of the ^{6}Li compounds. Now neutron captures occur in the beam pipe as often or even more often than captures in the crystals. Neutron capture on aluminum is now the most abundant reaction causing

TABLE 4. Ratio of events caused neutrons in the interval 10 .. 100 eV as a function of the energy deposition in the DANCE array. All numbers are relative to to the run with $^6Li_2CO_3$ plugs inside the ^{6}LiH neutron absorber, see Table 3 for absolute numbers.

Geometry	Total ratio	Ratio above 1 MeV	Ratio above 4 MeV
holes in ^{6}LiH	3.30	3.49	4.41
plugs in ^{6}LiH	1	1	1
no holes in ^{6}LiH	0.92	0.88	0.86

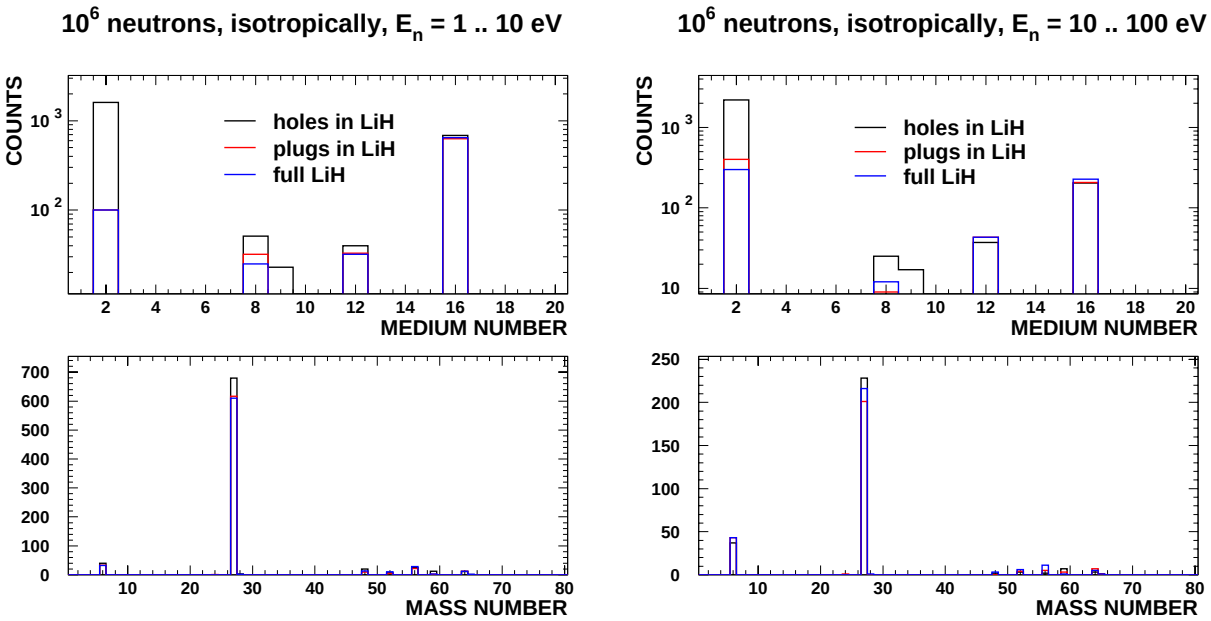

FIGURE 7. Number of neutron captures as a function of the medium as defined inside GEANT (top) and the mass of the capturing isotope, where BaF_2 is not considered (bottom). The left panel is for the neutron energy range 1 .. 10 eV and the right panel for 10 .. 100 eV.

a signal inside the DANCE array. This observation is confirmed by the lower panels of Fig. 7, where the number of counts is plotted as a function of the mass number of the isotope capturing the neutrons. BaF_2 is not contained in these plots, since it can not easily be replaced. Amongst the other isotopes, aluminum is by far the isotope with most captures.

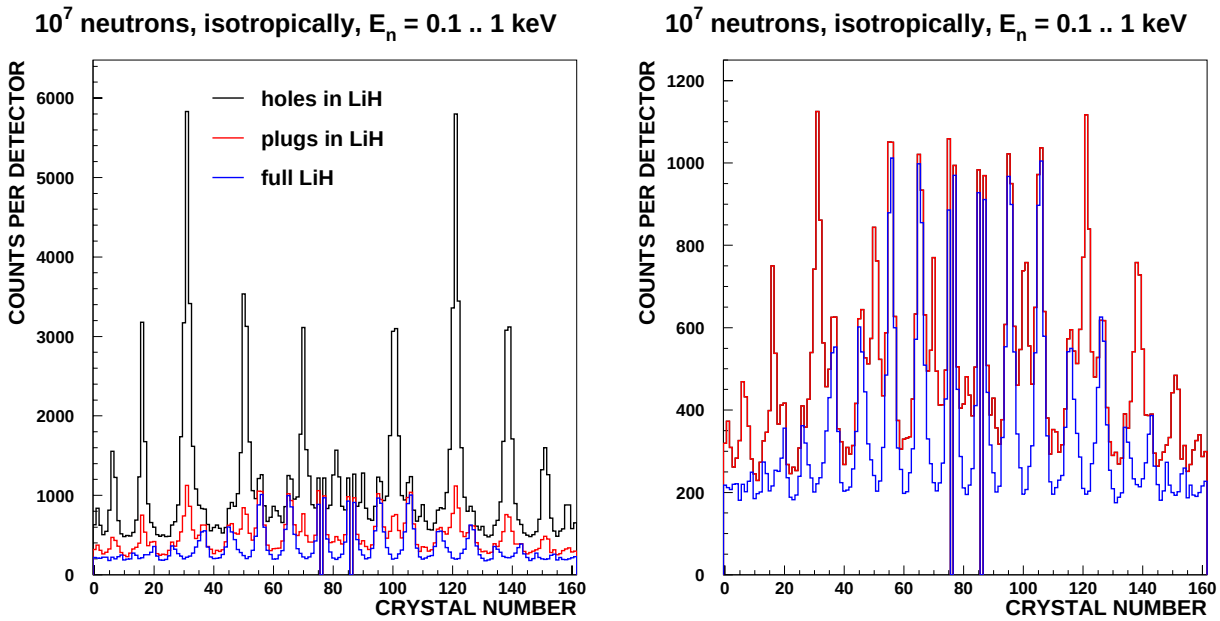

FIGURE 8. Number of events per detector for the neutron energy range 0.1 .. 1 keV for different geometries. The black curve corresponds to the setup as during the run 2004, where the neutron absorber contained holes for the sample changer. The red curve corresponds the a run with a plug of 3.5 cm $^6Li_2CO_3$ to fill the holes. Finally, the blue curve shows the result for a run with a plug of ^{6}LiH to fill the holes.

2.2. Medium neutron energies

The runs in this subsection are simulated with neutrons in the energy range between 0.1 and 10 keV. This is the region of unresolved resonances, which contributes significantly to the epithermal cross section. Furthermore, astrophysical applications require (n,γ) cross sections in the energy range between 1 and 200 keV. A strong suppression of background from scattered neutron is highly desirable, since the only possibility to distinguish between background and signal is via the energy and multiplicity information in the DANCE array. A separation of the two components based on the neutron energy is not possible anymore, since no resonances are resolved.

The neutron distribution within each run followed a $1/E_n$ spectrum, as it is typical for a spallation source. The additional plugs are less effective than for lower neutron energies. An reduction of the overall count rate due to neutrons, which are scattered off the sample, by a factor of more than two in the energy region of interest was observed. Furthermore, the difference between the $^6Li_2CO_3$ and the ^{6}LiH plugs is now increased to about 30%.

2.2.1. Events per Detector

Figs. 8 and 9 show the total number of counts per detector for the neutron energy interval 0.1-1 keV and 1-10 keV, respectively. Especially the number of counts in the detectors 31, 121 and their neighbors is largely reduced. The right part of each figure shows only the comparison between the two plugs.

Table 5 contains the total number of counts in different sum-energy regions for neutrons between 0.1 and 1 keV. Table 6 shows the same data, but normalized to the run with $^6Li_2CO_3$ plugs. At higher sum-energies, the $^6Li_2CO_3$ plugs are somewhat more effective and the difference between the $^6Li_2CO_3$ and the ^{6}LiH plugs is about 30%.

Tables 7 and 8 show the results for neutrons between 1 and 10 keV. The effect of the $^6Li_2CO_3$ is similar for this neutron energy range as for the one above.

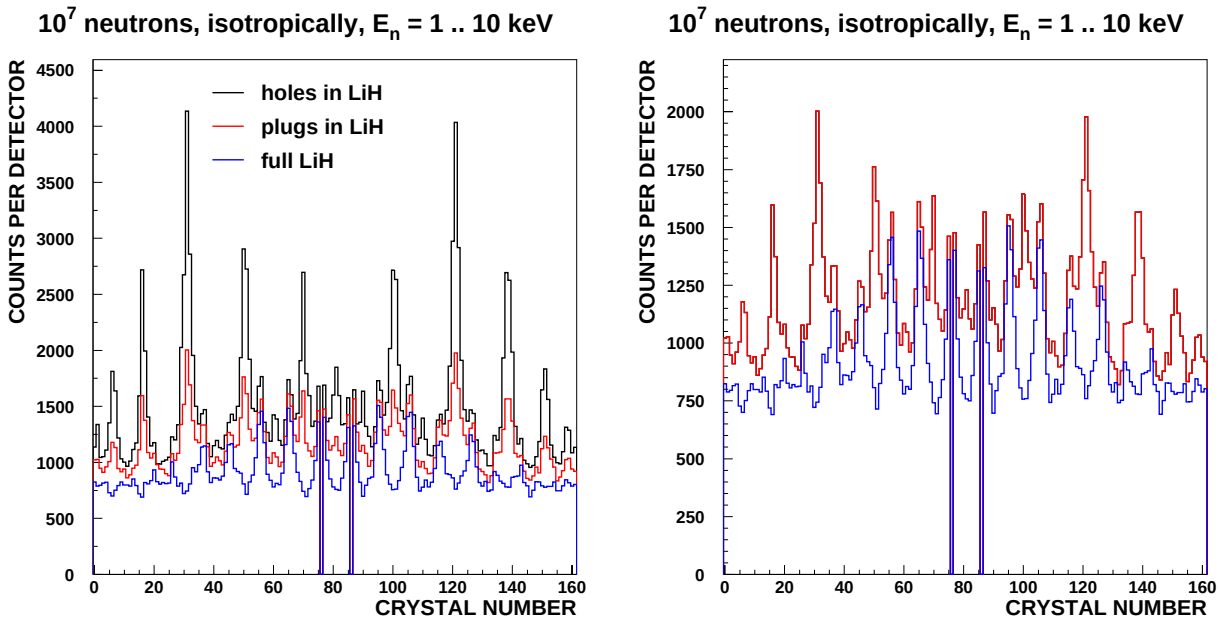

FIGURE 9. Number of events per detector for the neutron energy range 1 .. 10 keV for different geometries. The black curve corresponds to the setup as during the run 2004, where the neutron absorber contained holes for the sample changer. The red curve corresponds the a run with a plug of 3.5 cm $^6Li_2CO_3$ to fill the holes. Finally, the blue curve shows the result for a run with a plug of ^{6}LiH to fill the holes.

TABLE 5. Number of events caused by 10^7 neutrons in the interval 0.1 .. 1 keV as a function of the energy deposition in the DANCE array. The energy region above 4 MeV is most important for the experiments at DANCE.

Geometry	Total sum	Sum above 1 MeV	Sum above 4 MeV
holes in LiH	5.10 10^4	4.93 10^4	4.19 10^4
plugs in LiH	2.42 10^4	2.29 10^4	1.81 10^4
no holes in LiH	1.72 10^4	1.60 10^4	1.19 10^4

TABLE 6. Ratio of events caused neutrons in the interval 0.1 .. 1 keV as a function of the energy deposition in the DANCE array. All numbers are relative to to the run with $^6Li_2CO_3$ plugs inside the ^{6}LiH neutron absorber, see Table 5 for absolute numbers.

Geometry	Total ratio	Ratio above 1 MeV	Ratio above 4 MeV
holes in ^{6}LiH	2.11	2.15	2.31
plugs in ^{6}LiH	1	1	1
no holes in ^{6}LiH	0.71	0.70	0.66

TABLE 7. Number of events caused by 10^7 neutrons in the interval 1 .. 10 keV as a function of the energy deposition in the DANCE array. The energy region above 4 MeV is most important for the experiments at DANCE.

Geometry	Total sum	Sum above 1 MeV	Sum above 4 MeV
holes in LiH	6.80 10^4	6.59 10^4	5.66 10^4
plugs in LiH	5.39 10^4	5.21 10^4	4.42 10^4
no holes in LiH	4.23 10^4	4.06 10^4	3.39 10^4

TABLE 8. Ratio of events caused neutrons in the interval 1 .. 10 keV as a function of the energy deposition in the DANCE array. All numbers are relative to to the run with $^6Li_2CO_3$ plugs inside the ^{6}LiH neutron absorber, see Table 7 for absolute numbers.

Geometry	Total ratio	Ratio above 1 MeV	Ratio above 4 MeV
holes in ^{6}LiH	1.26	1.26	1.28
plugs in ^{6}LiH	1	1	1
no holes in ^{6}LiH	0.78	0.78	0.77

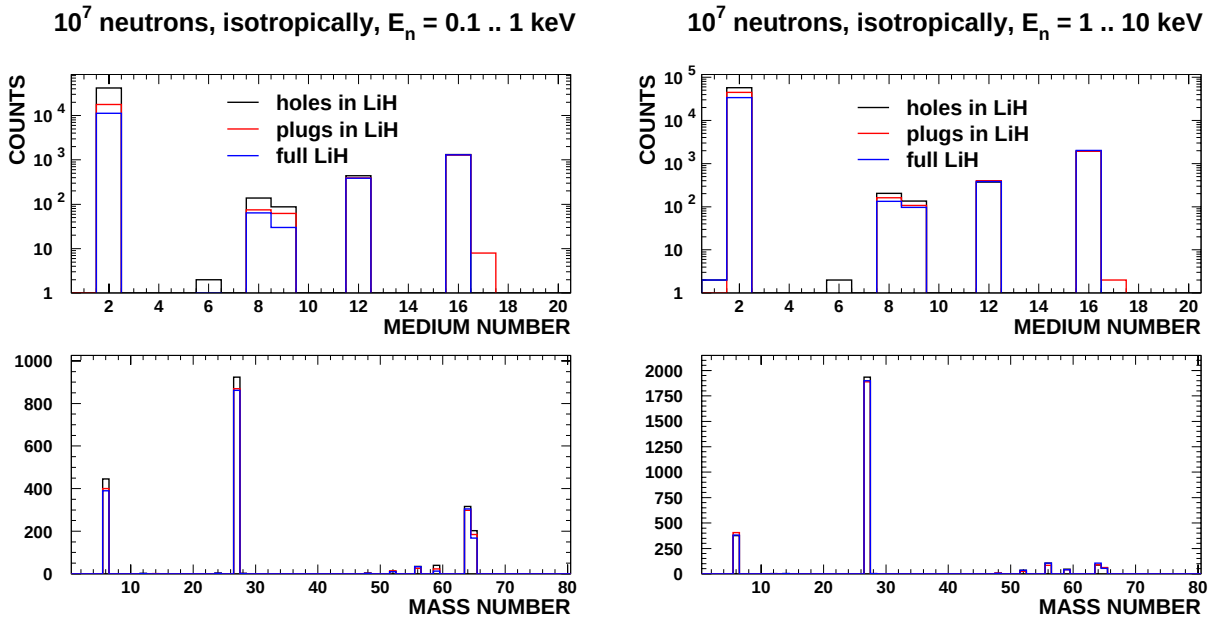

FIGURE 10. Number of neutron captures as a function of the medium as defined inside GEANT (top) and the mass of the capturing isotope, where BaF_2 is not considered (bottom). The left panel is for the neutron energy range 0.1 .. 1 keV and the right panel for 1 .. 10 keV.

2.2.2. Media and isotopes capturing neutrons

The two top panels of Fig. 10 show the number of neutron captures as a function of the medium number. With increasing energy, the effect of the beam pipe becomes less important. Most of the neutron captures occur inside the crystals (BaF_2), independent of the plugs. Apart from capture by BaF_2, neutron capture by aluminum is still the most abundant reaction causing a signal inside the DANCE array. This observation is confirmed by the lower panels of Fig. 10, where the number of counts is plotted as a function of the mass number of the isotope capturing the neutrons. BaF_2 is not contained in these plots, since it can not easily be replaced.

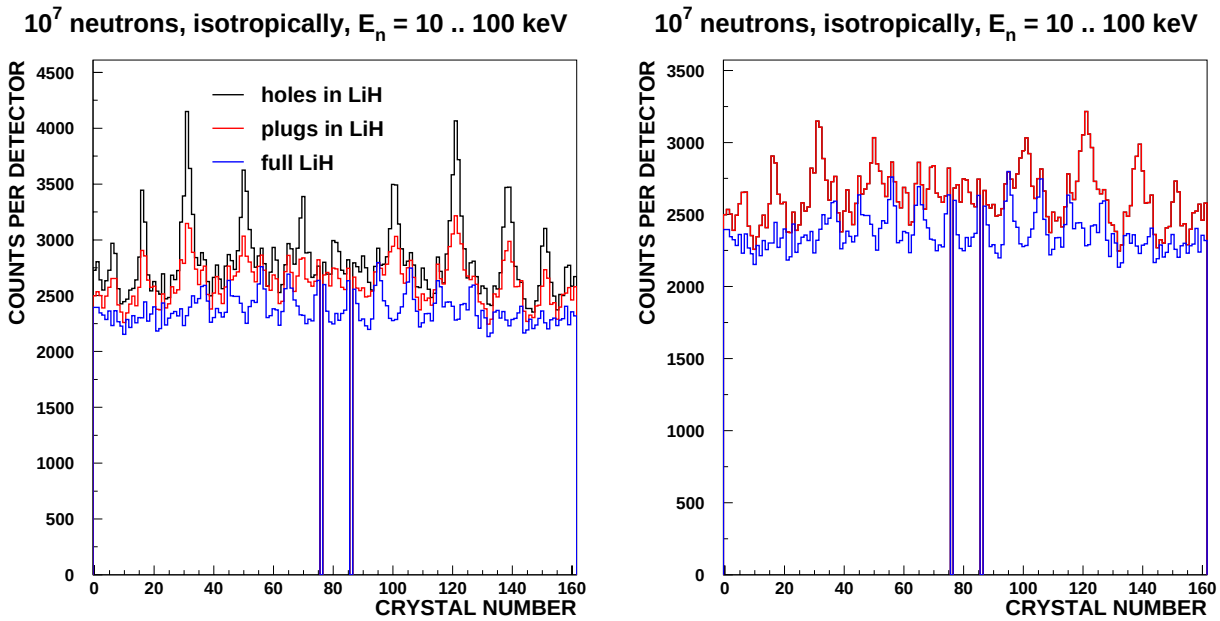

FIGURE 11. Number of events per detector for the neutron energy range 10 .. 100 keV for different geometries. The black curve corresponds to the setup as during the run 2004, where the neutron absorber contained holes for the sample changer. The red curve corresponds the a run with a plug of 3.5 cm $^6Li_2CO_3$ to fill the holes. Finally, the blue curve shows the result for a run with a plug of ^{6}LiH to fill the holes.

2.3. High neutron energies

The runs in this subsection are simulated with neutrons in the energy range between 10 keV and 1 MeV. The region between 10 and 100 keV is the most interesting energy range for astrophysical applications. A strong suppression of background from scattered neutrons is highly desirable, but difficult to achieve. The ratio of scattered to captured neutrons can easily exceed 10^3, which means that the signal is dominated by events due to scattered neutrons, if no suppression is possible.

The neutron distribution within each run followed a $1/E_n$ spectrum, as it is typical for a spallation source. The additional plugs are much less effective than for lower neutron energies. An reduction of the overall count rate due to neutrons, which are scattered of the sample, by 10% or less was observed. Furthermore, the the $^6Li_2CO_3$ plugs are in some sense half the way between no plugs at all and plugs made of ^{6}LiH.

2.3.1. Events per Detector

Figs. 11 and 12 show the total number of counts per detector for the neutron energy interval 10-100 keV and 0.1-1 MeV, respectively. Especially the number of counts in the detectors 31, 121 and their neighbors is reduced. The right part of each figure shows only the comparison between the two plugs.

Table 9 contains the total number of counts in different sum-energy regions for neutrons between 10 and 100 keV. Table 10 shows the same data, but normalized to the run with $^6Li_2CO_3$ plugs. At higher sum-energies, the $^6Li_2CO_3$ plugs are somewhat more effective and the difference between the three runs is about 10%.

Tables 11 and 12 show the results for neutrons between 0.1 and 1 MeV. The effect on the total number of counts is now almost negligible, it does not exceed a few percent.

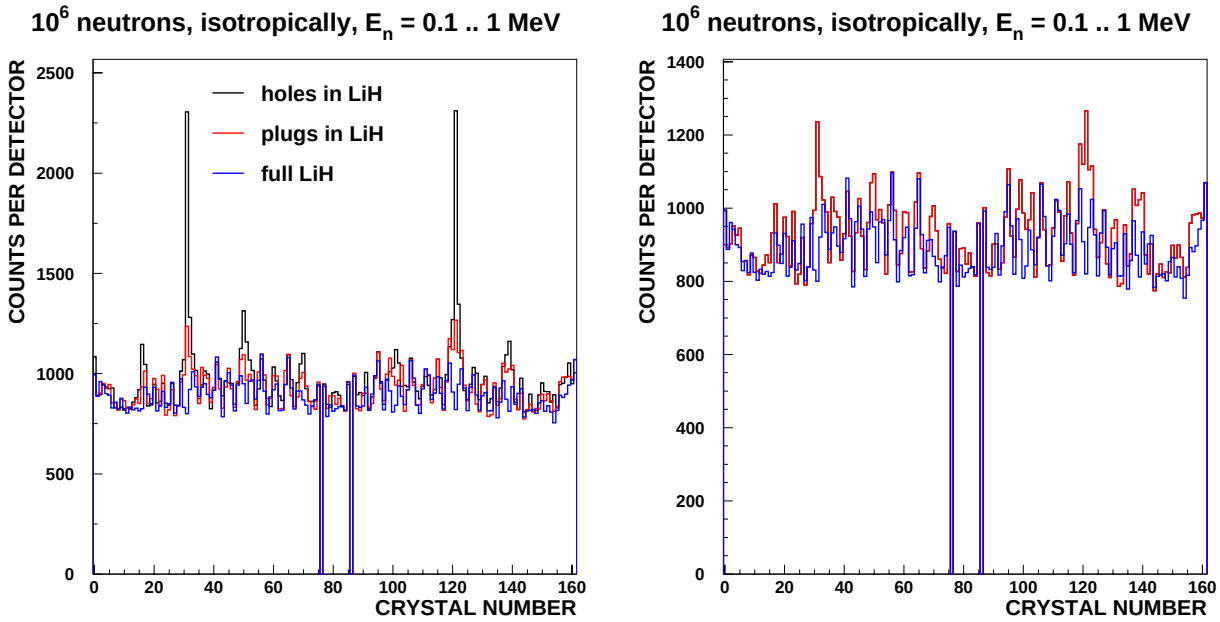

FIGURE 12. Number of events per detector for the neutron energy range 0.1 .. 1 MeV for different geometries. The black curve corresponds to the setup as during the run 2004, where the neutron absorber contained holes for the sample changer. The red curve corresponds the a run with a plug of 3.5 cm $^6Li_2CO_3$ to fill the holes. Finally, the blue curve shows the result for a run with a plug of ^{6}LiH to fill the holes.

TABLE 9. Number of events caused by 10^7 neutrons in the interval 10 .. 100 keV as a function of the energy deposition in the DANCE array. The energy region above 4 MeV is most important for the experiments at DANCE.

Geometry	Total sum	Sum above 1 MeV	Sum above 4 MeV
holes in LiH	1.26 10^5	1.23 10^5	1.08 10^5
plugs in LiH	1.18 10^5	1.15 10^5	1.01 10^5
no holes in LiH	1.06 10^5	1.03 10^5	9.08 10^4

TABLE 10. Ratio of events caused neutrons in the interval 10 .. 100 keV as a function of the energy deposition in the DANCE array. All numbers are relative to to the run with $^6Li_2CO_3$ plugs inside the ^{6}LiH neutron absorber, see Table 9 for absolute numbers.

Geometry	Total ratio	Ratio above 1 MeV	Ratio above 4 MeV
holes in ^{6}LiH	1.07	1.07	1.07
plugs in ^{6}LiH	1	1	1
no holes in ^{6}LiH	0.90	0.90	0.90

TABLE 11. Number of events caused by 10^6 neutrons in the interval 0.1 .. 1 MeV as a function of the energy deposition in the DANCE array. The energy region above 4 MeV is most important for the experiments at DANCE.

Geometry	Total sum	Sum above 1 MeV	Sum above 4 MeV
holes in LiH	8.55 10^4	1.97 10^4	1.73 10^4
plugs in LiH	8.14 10^4	1.93 10^4	1.70 10^4
no holes in LiH	7.85 10^4	1.86 10^4	1.63 10^4

TABLE 12. Ratio of events caused neutrons in the interval 0.1 .. 1 MeV as a function of the energy deposition in the DANCE array. All numbers are relative to to the run with $^6Li_2CO_3$ plugs inside the ^{6}LiH neutron absorber, see Table 11 for absolute numbers.

Geometry	Total ratio	Ratio above 1 MeV	Ratio above 4 MeV
holes in ^{6}LiH	1.05	1.02	1.02
plugs in ^{6}LiH	1	1	1
no holes in ^{6}LiH	0.96	0.96	0.96

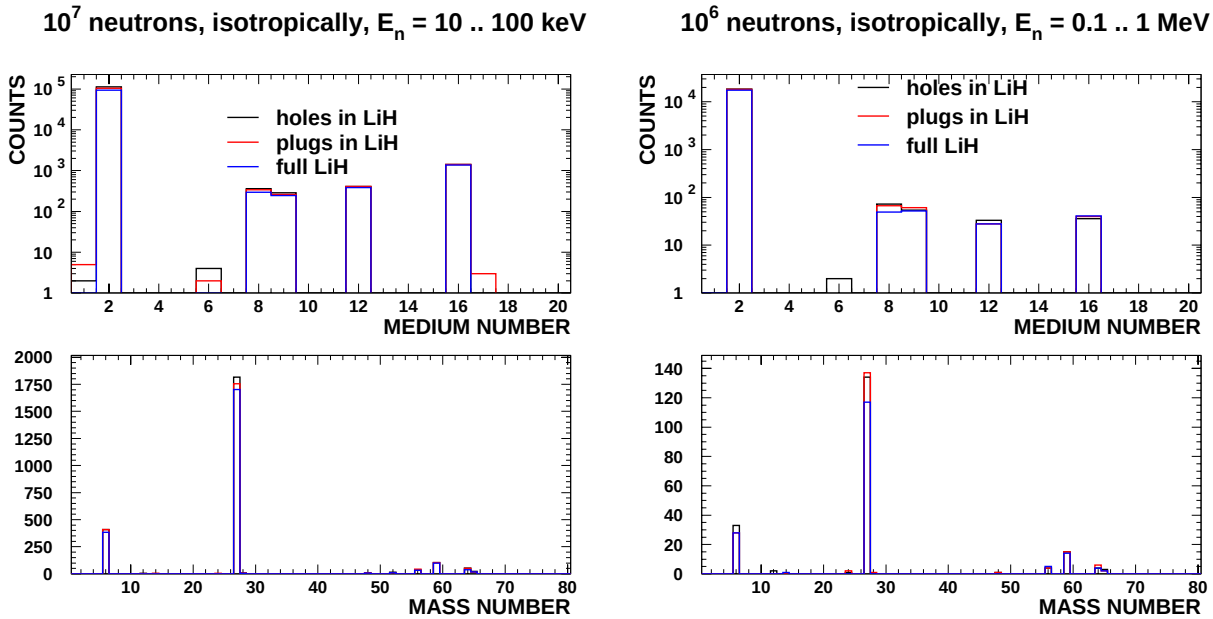

FIGURE 13. Number of neutron captures as a function of the medium as defined inside GEANT (top) and the mass of the capturing isotope, where BaF_2 is not considered (bottom). The left panel is for the neutron energy range 10 .. 100 keV and the right panel for 0.1 .. 1 MeV.

2.3.2. Media and isotopes capturing neutrons

The two top panels of Fig. 13 show the number of neutron captures as a function of the medium number. At these high energies, other structural components like the aluminum support structure and the photomultipliers are also contributing to the background. Most of the neutron captures still occur inside the crystals (BaF_2), independent of the plugs. Apart from capture by BaF_2, neutron capture by aluminum is the most abundant reaction causing a signal inside the DANCE array. This observation is confirmed by the lower panels of Fig. 13, where the number of counts is plotted as a function of the mass number of the isotope capturing the neutrons. BaF_2 is not contained in these plots, since it can not easily be replaced. see Fig. 13

3. THE NEUTRON ABSORBER AND GAMMAS

As already discussed above, the additional plugs will not only affect the scattered neutrons, but also the γ-rays following a neutron capture by the sample on their way to the BaF_2 crystals. In order to investigate this effect, a set of simulations has been performed, where 10^6 γ-rays of different energies where isotropically emitted from the center of the DANCE array. The impact of $^6Li_2CO_3$ of different thicknesses on the energy deposition in the BaF_2 crystals was then investigated.

Figures 14 to 20 show the results for plug thicknesses of 2 cm and 3.5 cm.

- The left panel of each figure shows the simulated sum-energy.
- The middle panel of each figure shows the energy deposition for crystal 31, which is together with crystal 121 the most affected crystal.
- The right panel of each figure shows the energy deposition for crystal 0, which should not be affected by the plugs.

The result is twofold:

1. For gamma-energies below 1 MeV, the response of the single detectors in front of the plugs depends on the thickness of the plugs. The 2 cm thick $^6Li_2CO_3$ plug has approximately the same effect on γ-rays as 6 cm of ^6LiH.
2. The sum-energy spectrum of the entire ball is basically not affected by the insertion of the plugs, independent of the γ-energy.

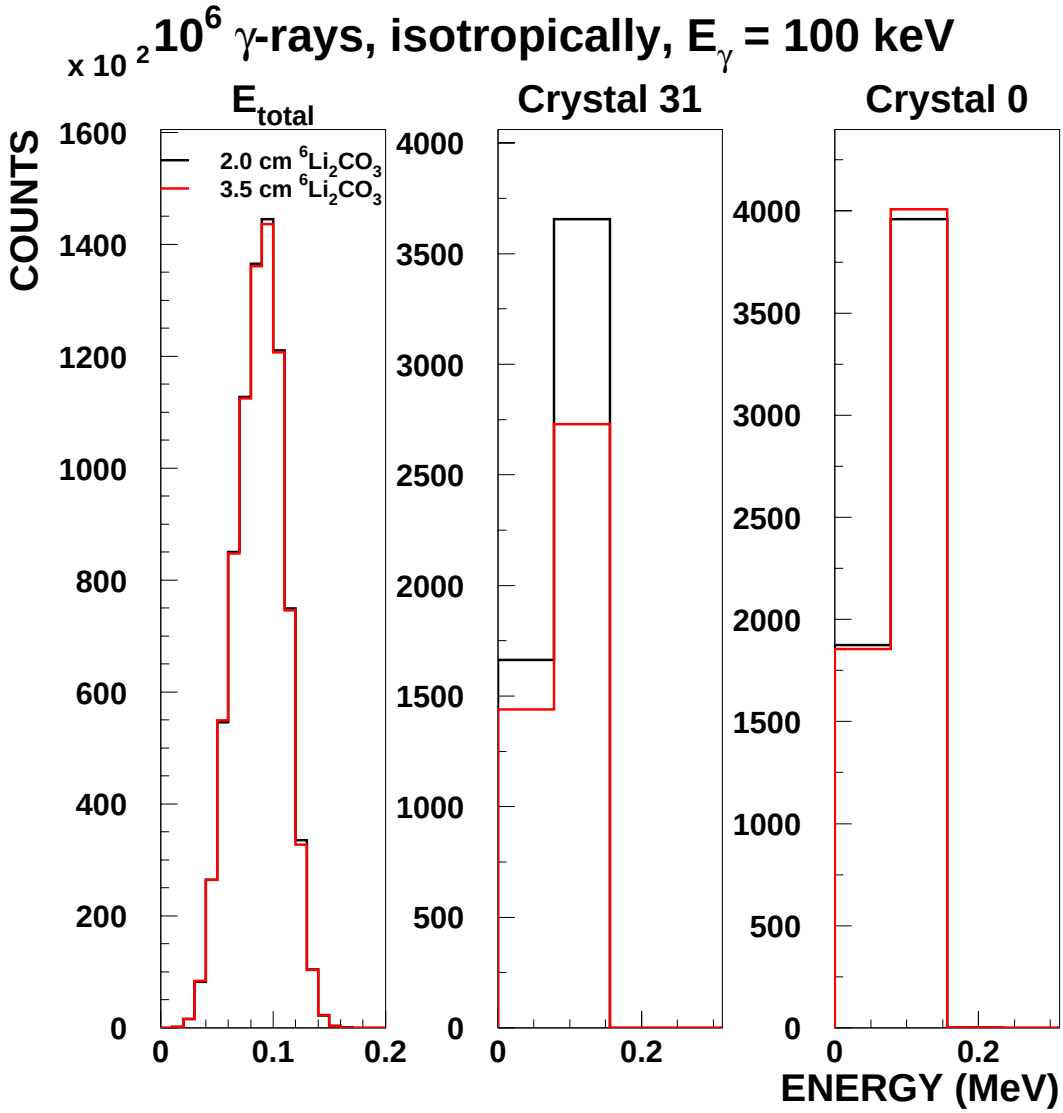

FIGURE 14. All three spectra are the result of the simulation of 10^6 γ-rays with an energy of 0.1 MeV. Left: Total energy deposited in the DANCE array for two different plug thicknesses (2.0 and 3.5 cm). Middle: Energy spectra for crystal number 31, which was most effected by the change of the plug thickness. Right: The energy spectra of crystal number 0 are shown for comparison with the middle panel.

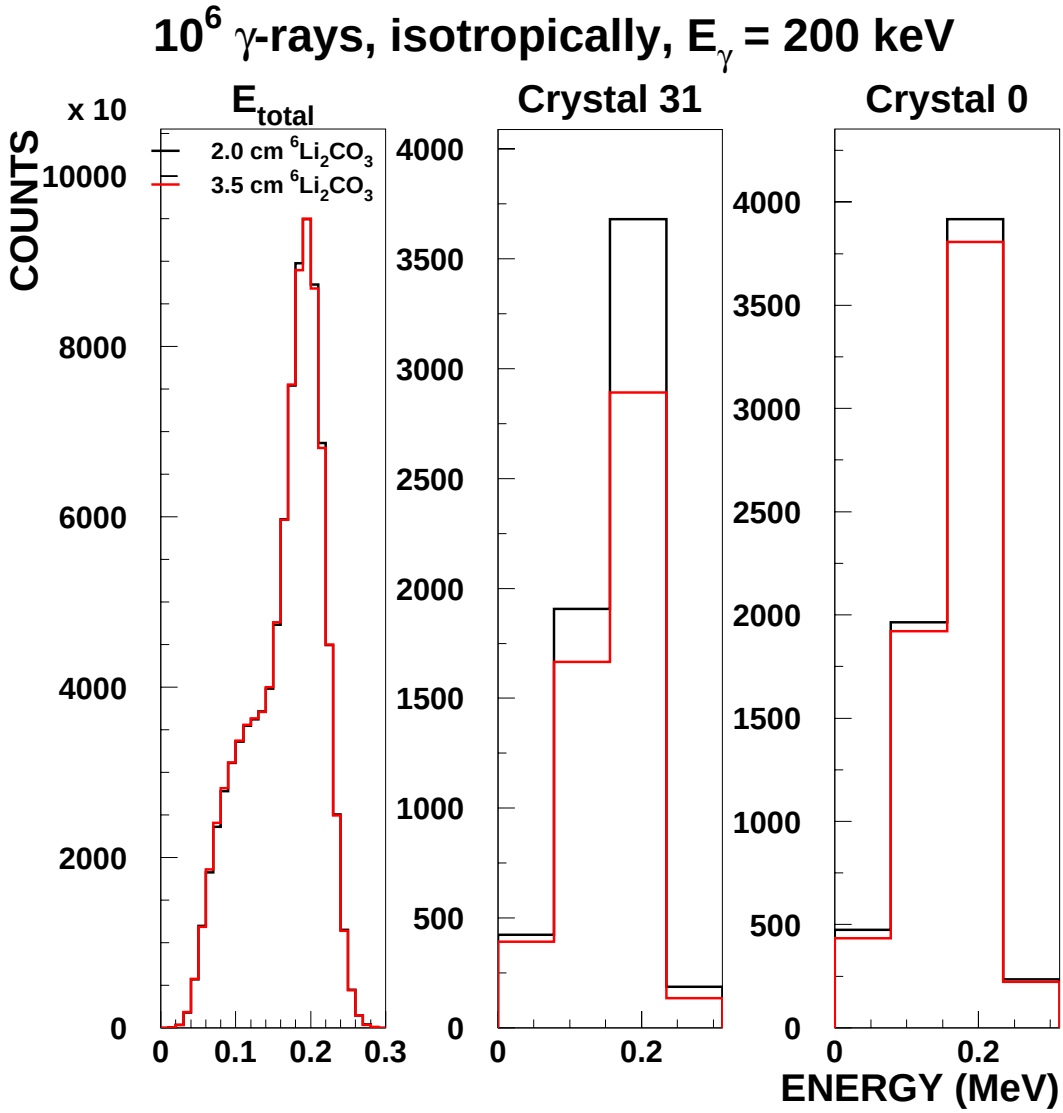

FIGURE 15. All three spectra are the result of the simulation of 10^6 γ-rays with an energy of 0.2 MeV. Left: Total energy deposited in the DANCE array for two different plug thicknesses (2.0 and 3.5 cm). Middle: Energy spectra for crystal number 31, which was most effected by the change of the plug thickness. Right: The energy spectra of crystal number 0 are shown for comparison with the middle panel.

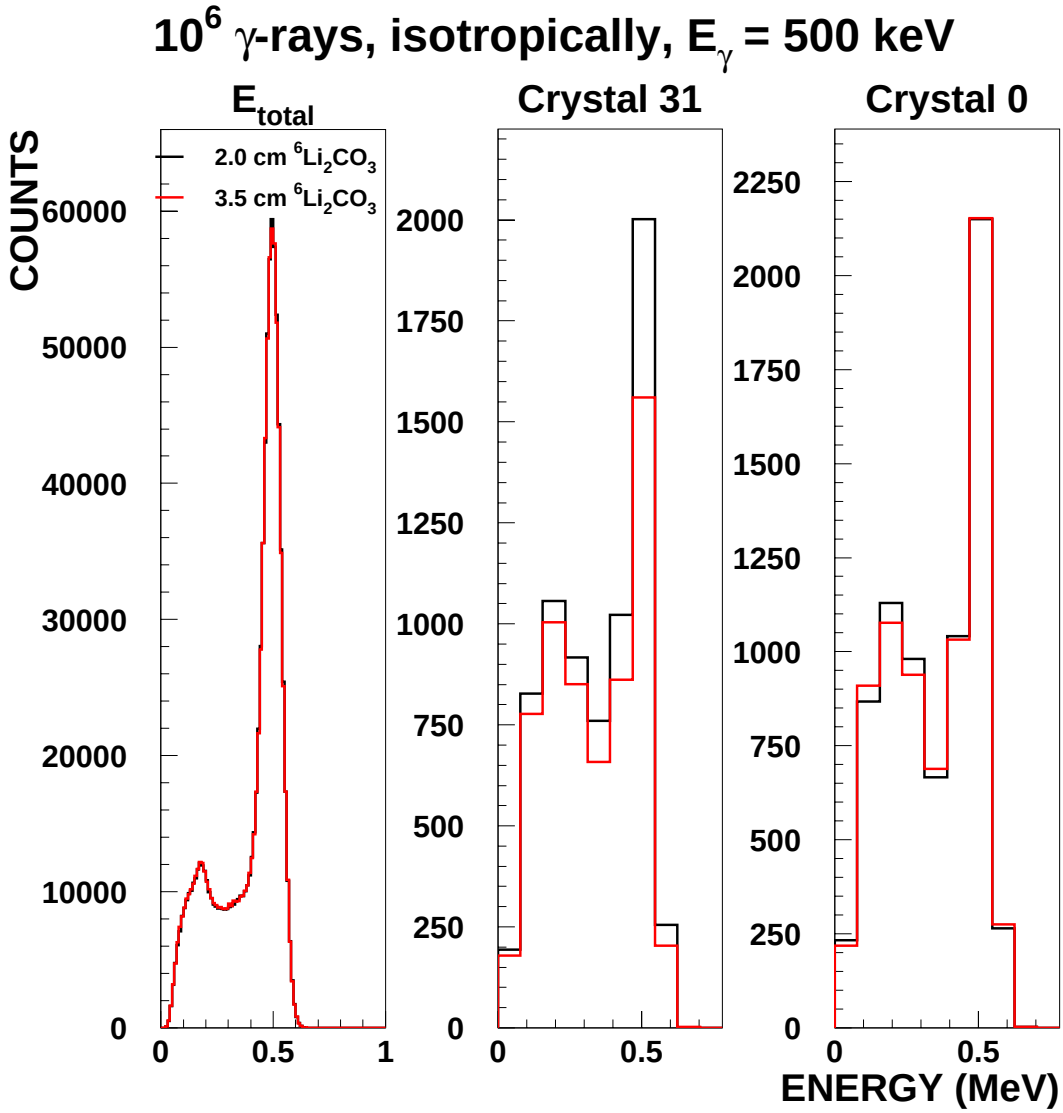

FIGURE 16. All three spectra are the result of the simulation of 10^6 γ-rays with an energy of 0.5 MeV. Left: Total energy deposited in the DANCE array for two different plug thicknesses (2.0 and 3.5 cm). Middle: Energy spectra for crystal number 31, which was most effected by the change of the plug thickness. Right: The energy spectra of crystal number 0 are shown for comparison with the middle panel.

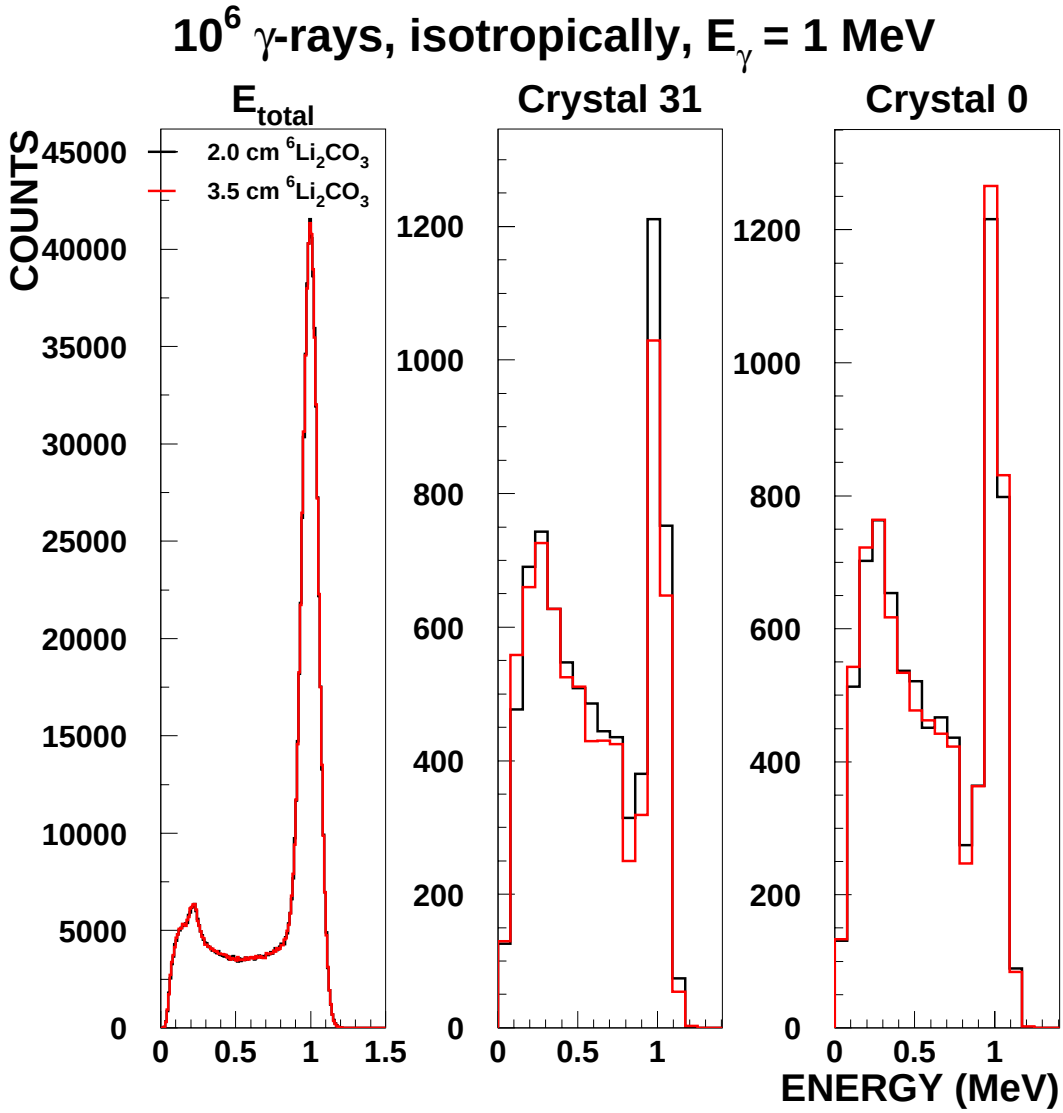

FIGURE 17. All three spectra are the result of the simulation of 10^6 γ-rays with an energy of 1 MeV. Left: Total energy deposited in the DANCE array for two different plug thicknesses (2.0 and 3.5 cm). Middle: Energy spectra for crystal number 31, which was most effected by the change of the plug thickness. Right: The energy spectra of crystal number 0 are shown for comparison with the middle panel.

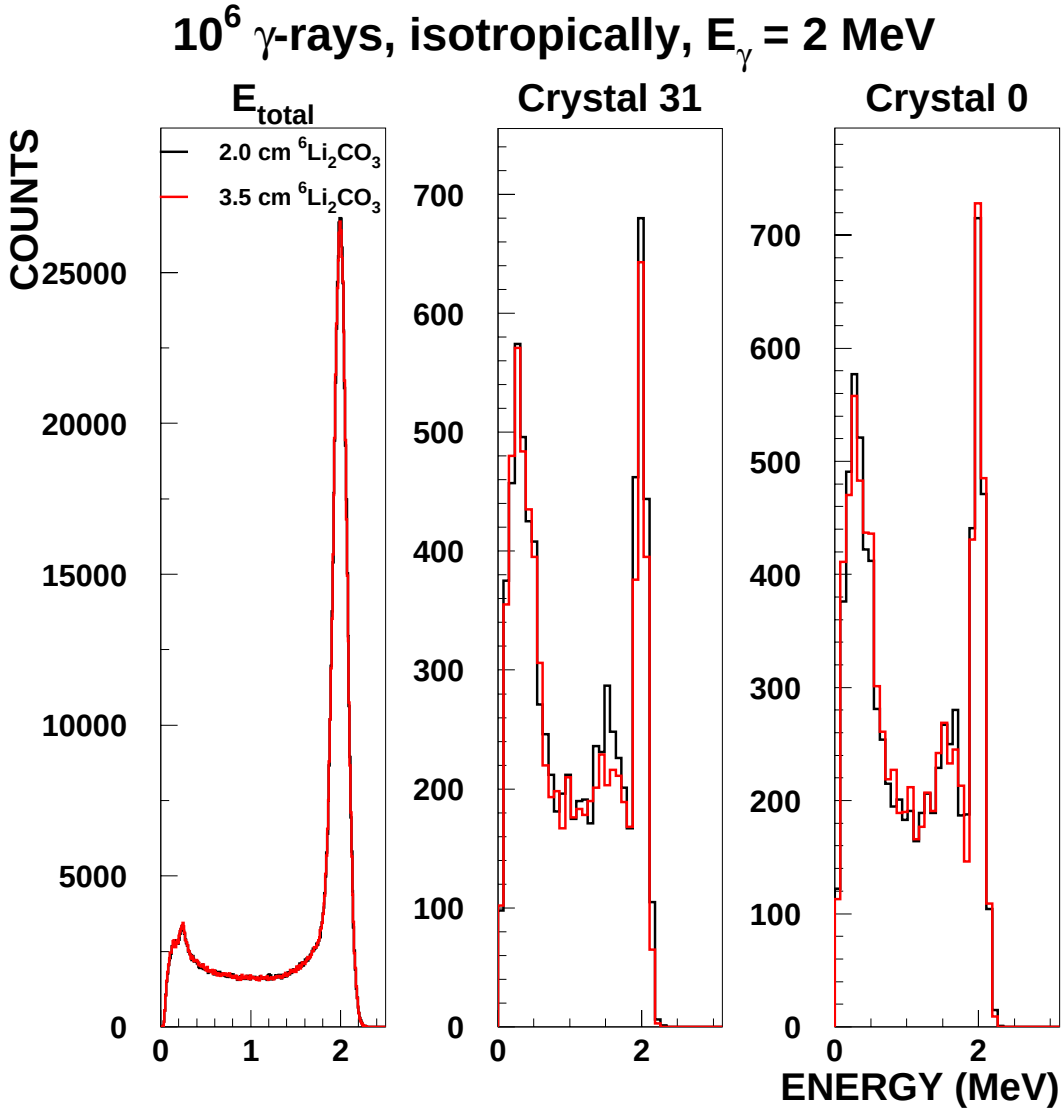

FIGURE 18. All three spectra are the result of the simulation of 10^6 γ-rays with an energy of 2 MeV. Left: Total energy deposited in the DANCE array for two different plug thicknesses (2.0 and 3.5 cm). Middle: Energy spectra for crystal number 31, which was most effected by the change of the plug thickness. Right: The energy spectra of crystal number 0 are shown for comparison with the middle panel.

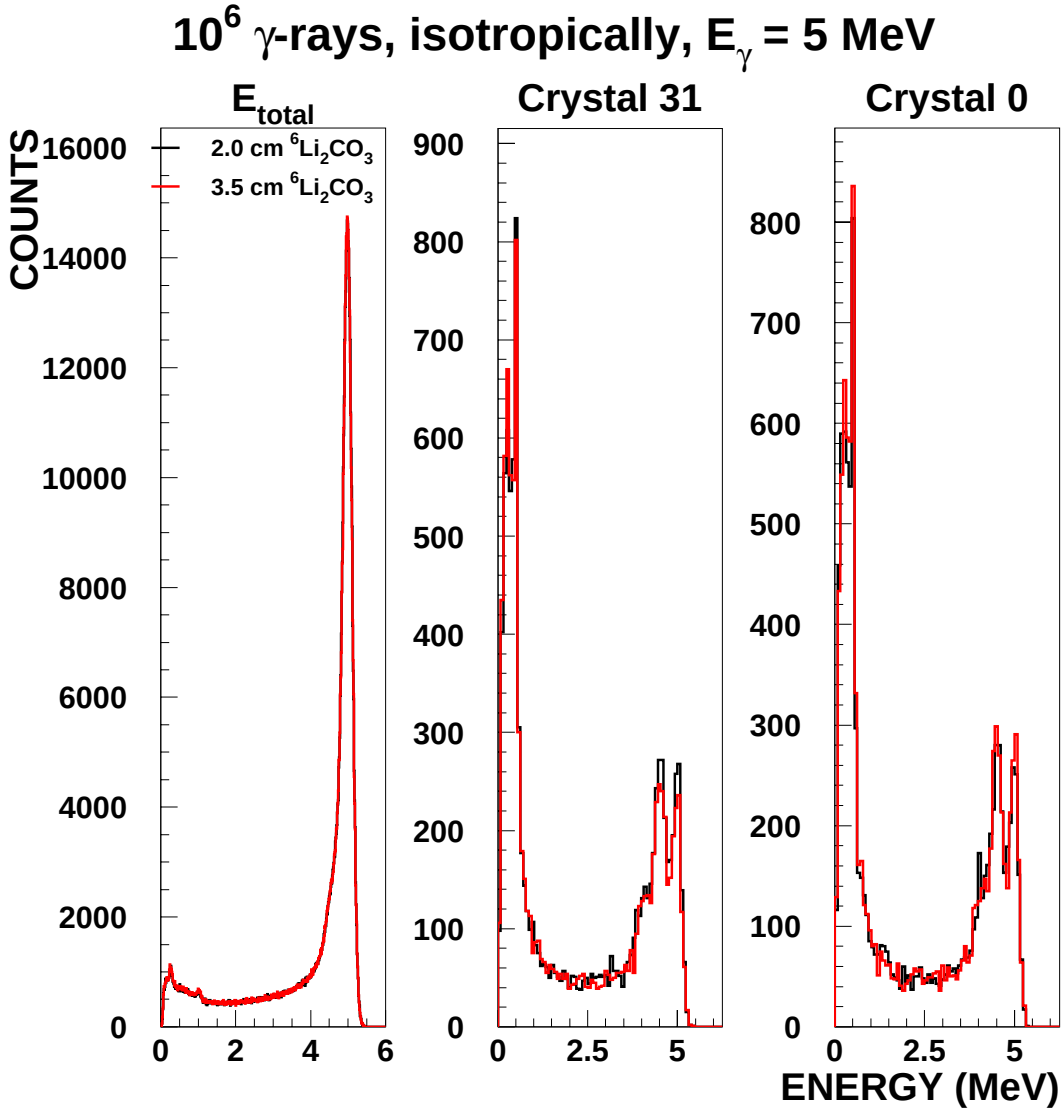

FIGURE 19. All three spectra are the result of the simulation of 10^6 γ-rays with an energy of 5 MeV. Left: Total energy deposited in the DANCE array for two different plug thicknesses (2.0 and 3.5 cm). Middle: Energy spectra for crystal number 31, which was most effected by the change of the plug thickness. Right: The energy spectra of crystal number 0 are shown for comparison with the middle panel.

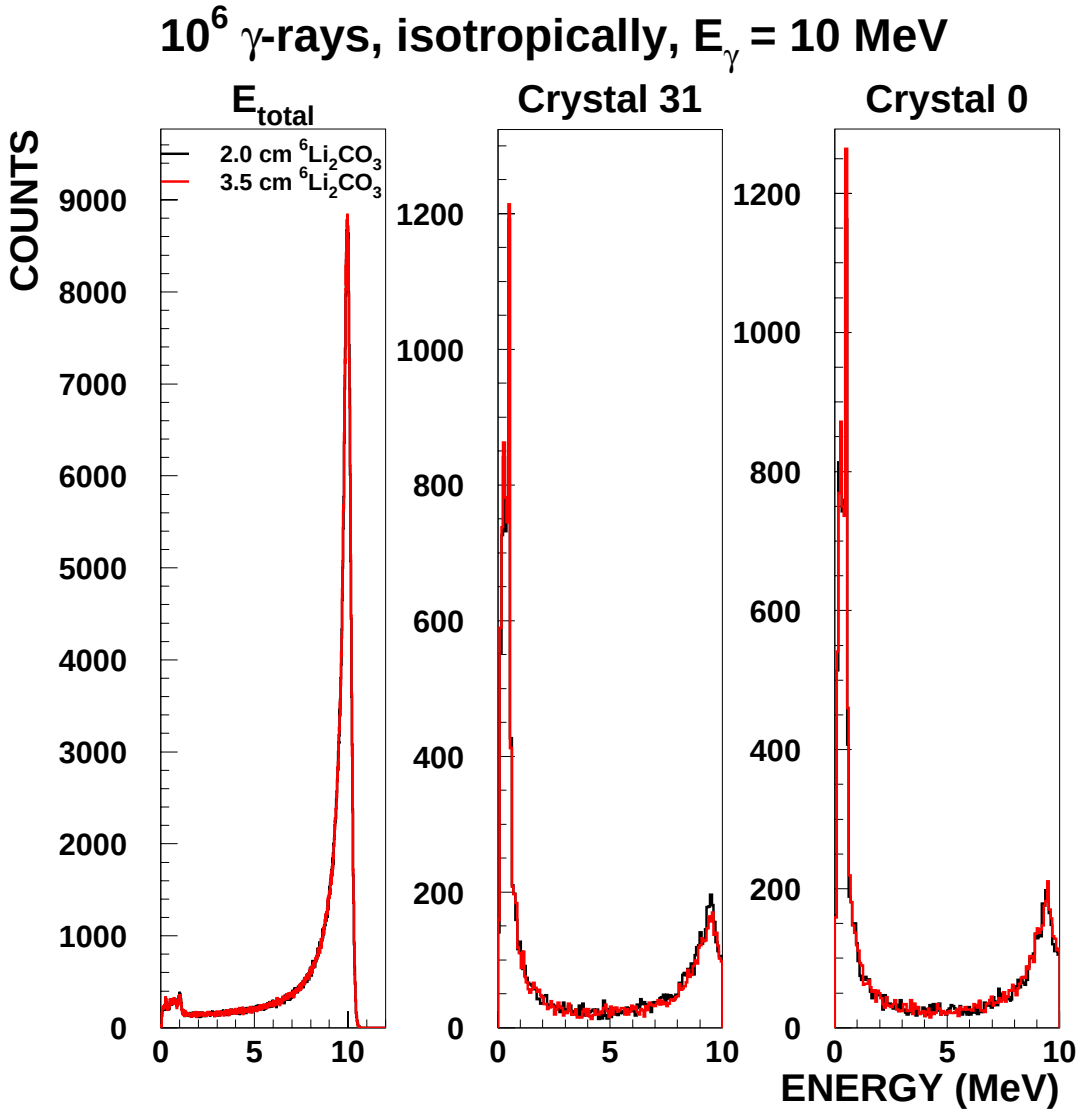

FIGURE 20. All three spectra are the result of the simulation of 10^6 γ-rays with an energy of 10 MeV. Left: Total energy deposited in the DANCE array for two different plug thicknesses (2.0 and 3.5 cm). Middle: Energy spectra for crystal number 31, which was most effected by the change of the plug thickness. Right: The energy spectra of crystal number 0 are shown for comparison with the middle panel.

4. CONCLUSION

Numerous simulations with the detector simulation package GEANT have been performed to investigate the need of filling the holes in the neutron absorber shell inside the DANCE array. The simulations have shown that it is not necessary to buy the expensive ^{6}LiH plugs, but that plugs made of the much cheaper $^6Li_2CO_3$ have a similar effect. We therefore recommend to fill the holes with 3.5 cm plugs of $^6Li_2CO_3$.

Another important result was that, especially for neutron energies below 1 keV, neutron captures by aluminum inside the beam pipe are the strongest source of neutron induced background, as soon as the holes in the absorber shell are filled with a ^{6}Li compound. We therefore recommend to thoroughly investigate the possibility of using different materials for the beam pipe. Possible candidates are carbon fiber or beryllium.

ACKNOWLEDGMENTS

This work has benefited from the use of the Los Alamos Neutron Science Center at the Los Alamos National Laboratory. This facility is funded by the US Department of Energy and operated by the University of California under Contract W-7405-ENG-36.

REFERENCES

1. Reifarth, R., Bredeweg, T., Alpizar-Vicente, A., Browne, J., Esch, E., Greife, U., Haight, R., Hatarik, R., Kronenberg, A., O'Donnell, J., , Rundberg, R., Ullmann, J., Vieira, D., Wilhelmy, J., and Wouters, J., *Nucl. Instr. Meth. A*, **531**, 528 (2004).
2. Reifarth, R., Heil, M., Käppeler, F., Voss, F., Wisshak, K., Haight, R., Dragowsky, M., Fowler, M., Rundberg, R., Ullmann, J., Wilhelmy, J., and Seabury, E., New geant simulations of neutron capture experiments with a 4π baf_2 detector, Tech. rep., Report LA-UR-01-4185, Los Alamos National Laboratory (2001).
3. Reifarth, R., Bredeweg, T., Browne, J., Esch, E., Greife, U., Haight, R., O'Donnell, J., Kronenberg, A., , Rundberg, R., Ullmann, J., Vieira, D., Wilhelmy, J., and Wouters, J., Results of geant simulations and comparison with first experiments at dance, Tech. rep., Report LA-UR-03-5560, Los Alamos National Laboratory (2003).
4. Reifarth, R., Esch, E., Haight, R., and Ullmann, J., An independent method for determining cascade efficiencies of the dance array, Tech. rep., Report LA-UR-03-9227, Los Alamos National Laboratory (2003).
5. Apostolakis, J., Cern program library long writeup, w5013, Tech. rep., CERN, GEANT library (1993), http://wwwinfo.cern.ch/asd/geant/.